Supplementary data

Supplementary Figure legends

Fig. S1. Structural comparison of the *Xl*Nse1-3-4 complex and the *Hs*Nse1-Nse3 complex.

(a) Structural comparison of the *Xl*Nse1-3-4 and *Hs*Nse1-Nse3 by aligning Nse1 (orange). Nse3 and Nse4 are colored green and blue, respectively. The *Xl*Nse1-3-4 structure is similar to the closed form of *Hs*Nse1-Nse3 (PDB 3NW0), in which the WHA and WHB of Nse3 are located close to each other. In the open form of *Hs*Nse1-Nse3 (PDB 5HVQ), the WHA and WHB of Nse3 are distantly located.

(b) The extended L2'' loop of Nse4 (blue) passes through the interface between Nse1 (orange) and Nse3 (green). The L2'' loop enters a channel formed by the L1A' loop, the S2A' and S3A' strands, the H1B' and H4B' helices, and the WHA-WHB linker of Nse3 (left), and exits a channel formed by the S3A strand; the H1B, H3B, and H4B helices; the L3B loop; and a WHA-WHB linker of Nse1 (right).

Fig. S2. Structure-based sequence alignment of KITE proteins Nse1, ScpB and MukE. Highly conserved and moderately conserved residues are highlighted in orange and light orange, respectively. Helices and strands are indicated as cylinders and arrows, respectively. The segments lacking the regular secondary structure are represented as solid lines. The secondary structures of *Ec*MukE are indicated as solid lines below its sequence. Residues involved in DNA binding are highlighted with red stars [1], and residues binding Nse4 and Zn ions are marked by blue or black circles, respectively. The green circle indicates the Nse3-binding residues in previous yeast-two hybrid analysis [2]. Every 10 residues of *Xl*Nse1 are marked by vertical bar. PROMALS3D was used for alignment of Nse1 from frog (*Xenopus laevis,* Uniprot entry: Q6PAF4), budding yeast (*Saccharomyces cerevisiae,* Q07913), fission yeast (*Schizosaccharomyces pombe,* Q53EK2), human (*Homo sapiens,* Q8WV22), cow (*Bos Taurus,* Q3T0X7), pig (*Sus scrofa,* A0A286ZS01), mouse (*Mus musculus,* A0A0R4J0C0), chicken (*Gallus gallus,* E1BWX7), fruit fly (*Drosophila melanogaster,* Q9VMA0), ScpB from Bs (*Bacillus subtilis,* P35155), Gs (*Geobacillus stearothermophilus,* A0A0K2HBM0), Pf (*Pyrococcus furiosus,* A0A5C0XSN0), Sp (*Streptococcus pneumonia,* Q97NX6) and Ec (*Escherichia coli*) MukE (P22524).

Fig. S3. Structure-based sequence alignment of KITE proteins Nse3, ScpB and MukE. Residues involved in DNA binding are highlighted with red stars [1]. Residues involved in Nse4 binding are colored blue (this study) or represented by yellow circles from Y2H [3]. The black and green indicates the mutation sites that increase sensitivity to DNA damage agents [3, 4]. PROMALS3D was used for alignment of Nse1 from frog (*Xenopus laevis,* A0A1L8G3Z0), budding yeast (*Saccharomyces cerevisiae,* Q05541), fission yeast (*Schizosaccharomyces pombe,* Q9Y7U4), human (*Homo sapiens,* Q96MG7), cow (*Bos Taurus,* Q0D253), pig (*Sus scrofa,* F1SNQ4), mouse (*Mus musculus,* Q9CPR8), chicken (*Gallus gallus,* Q001T8), fruit fly (*Drosophila melanogaster,* Q9VMA0), ScpB from Bs (*Bacillus subtilis,* P35155), Gs (*Geobacillus stearothermophilus,* A0A0K2HBM0), Pf (*Pyrococcus furiosus,* A0A5C0XSN0), Sp (*Streptococcus pneumonia,* Q97NX6) and Ec (*Escherichia coli*) MukE (P22524).

Fig. S4. Structure-based sequence alignment of kleisin proteins Nse4 and ScpA. Disordered regions are illustrated as dotted lines. The N-terminal HTH motif and C-terminal WH domain are boxed. Residues involved in DNA binding are highlighted by red stars. Residues binding Nse1 or Nse3 are marked by yellow or green circles, respectively. The black circles indicate the Nse3-binding residues in previous studies [5]. The Δ indicates deletion of the marked region, which impaired the interaction of Nse4 with Nse3 in fission yeast [2]. PROMALS3D was used for alignment of Nse1 from frog (*Xenopus laevis,* B1WBD6), budding yeast (*Saccharomyces cerevisiae,* P43124), fission yeast (*Schizosaccharomyces pombe,* Q6BDR8), human (*Homo sapiens,* Q8N140), cow (*Bos taurus,* A6QPC8), pig (*Sus scrofa,* I3L6I0), mouse (*Mus musculus,* Q3V124), chicken (*Gallus gallus,* F1NV66), and fruit fly (*Drosophila melanogaster,* Q9VKV4), and ScpB from Bs (*Bacillus subtilis,* P35154), Gs (*Geobacillus stearothermophilus,* A0A0K2HBN1), Pf (*Pyrococcus furiosus,* Q8TZY3) and Sp (*Streptococcus pneumonia,* Q97NX5).

Fig. S5. The interfaces between Nse4 and the Nse1-Nse3 complex

(a) The first interface between the H1'' helix of Nse4 (blue) and WHB of Nse3 (green) in same view of Fig. 3b. The H1'' helix of Nse4 is surrounded by the H1B', H2B' and H5B' helices of

Nse3.

(b) The second interface between the H2'' helix of Nse4 (blue) and the H1B' and H5B' helices of Nse3 (green) in same view of Fig 3c.

(c) The third interface between Nse4 (the extended loop) and the Nse1-Nse3 complex in same view of Fig. 3d.

Fig. S6. Comparison of the Nse1-3-4 complex with ScpAB and MukEF.

(a) Cylinder representation of *Sp*ScpAB. The WHA of ScpB (orange) is aligned with WHA of *Xl*Nse1 in Fig. 4a. The H5 helix of ScpA (blue) which is not observed in Nse1-3-4 complex or MukEF passes through the groove formed by H1B, H4B and H5B of ScpB (orange and magenta) and H3B' of ScpB' (white).

(b) Surface representation of *Sp*ScpAB in same view with (a). The helices of ScpB (light orange) and ScpB' (white) equivalent to the helices of Nse1 and Nse3 are shown in red and black cylinder, respectively. ScpA is colored blue. The WHB C-terminal extension of both ScpB and ScpB' are colored magenta.

(c) Close-up view of the *Sp*ScpA (blue)-ScpB' (white) interface. A long helix of ScpA is perpendicular to the H1B' helix of ScpB'.

(d) Close-up view of the path of the L2'' loop of Nse4 (blue). The loop passes through the interface of Nse1 (orange)-Nse3 (white).

(e) Close-up view of the path of the loop in *Gs*ScpA equivalent to the L2'' loop of Nse4. WHA of ScpB' (white) is aligned with WHA of Nse3 in (d).

(f) Close-up view of the path of the loop in *Sp*ScpA equivalent to the L2'' loop of Nse4.

(g) Close-up view of the path of the loop in *Ec*MukF equivalent to the L2'' loop of Nse4. WHA of MukE' (white) is aligned with WHA of Nse3 in (d).

Fig. S7. A model of the N-terminal region of Nse4

(a) A model of Nse4ML C-tail (residues 187 to 211) of Nse4 based on the ScpAB structure

(PDB 3W6J) [6]. Nse1, Nse3 and Nse4 are colored bright orange, white and blue, respectively. In the structural alignment of WHA of Nse3 and ScpB', the C-terminal region of *Gs*ScpA (green) collides with the H1B' and H3B' helices of Nse3. The green helix moves toward the cyan helix (indicated by an arrow) to mimic the H6 helix in *Gs*ScpA (or the H5 helix of *Sp* ScpA). The Nse4ML C-tail (cyan) is located in a groove formed by two WHBs of Nse1 and Nse3. All dotted lines indicate crosslinks of the residues from CL-MS^{NSE} [7]. However, in a model shown here, the Cα atoms connected by the dotted lines are separated over 30 Å. Residues in human Nse3, and Nse4 equivalent to those of *Xl*NSE proteins are marked inside the parenthesis.

(b) Model of the N-terminal region of Nse4 (residues 30 to 104) and Nse4ML C-tail (residues 187 to 211) based on CL-MS^{NSE}. Nse1 (bright orange), Nse3 (white), and Nse4 (blue) are shown in cylinder representation. The modelled N- and C-terminal regions are colored cyan. Residues in human Nse3, and Nse4 equivalent to those of *Xl*NSE proteins are marked inside the parenthesis. Yellow and blue spheres indicates the crosslinking range of Lys160 and Glu231 of Nse3, respectively. Lys100 of Nse4 is likely to be within the overlapping region of two spheres. Lys100 of Nse4 is within crosslinking distance of Lys160 and Glu231 of Nse3 in our model (solid line).

Fig. S8. DNA-binding of various forms of the *Xl*Nse1-3-4 complex.

(a) Analysis of DNA binding between various Nse1-3-4 complexes and a 5'-FAM-labelled 37 bp dsDNA. Numbers at the top of the gels indicate the Nse4 constructs used for analysis. Nse1 (residues 3 to 248) and Nse3 (residues 45 to 260) were used for all DNA-binding analyses. Each protein was incubated with 5'-FAM-labelled 37 bp dsDNA (0.2 μM) for 30 min on ice with increasing molar concentrations of proteins. The protein molar concentration (0.2 ~ 45 μM) are indicated at the top of each gel. On top, cartoons show Nse1 (orange), Nse3 (green) and Nse4 (blue).

(b) Analysis of DNA binding between Nse1-3-4 complexes containing Nse3 or Nse4 mutants and a 5'-FAM-labelled 37 bp dsDNA. Nse1 (residues 3 to 248), Nse3 (residues 45 to 260), and Nse4 (residues 30 to 220) constructs were used for all mutants. Reaction conditions were the same as in (a). Nse3 mutant, K187E/K195E; Nse4 N mutant, R33E/R35E/R38E/R52E; Nse4

C1 mutant, K187E/K198E/K211E; Nse4 C2 mutant, R192E/K194E/R195E; Nse4 C3 mutant, C1+C2.

(c) Electrostatic surface potential representation of the DNA-bound Nse1-3-4 model. The electrostatic potential was calculated by APBS [8] and displayed using Pymol. Positively and negatively charged regions are colored blue and red, respectively.

(d) Analysis of DNA binding between the Smc6 (residues 85 to 299 and 925 to 1107)-Nse1 (residues 3 to 248)-Nse3 (residues 45 to 260)-Nse4 (residues 30 to 183, left or 30 to 220, right) complex and a 5'-FAM-labelled 37 bp dsDNA. Reaction conditions were the same as those in (a).

(e) Analysis of DNA binding between the Smc6 (residues 85 to 299 and 925 to 1107)-Nse1 (residues 3 to 248)-Nse3 (residues 45 to 260)-Nse4 (residues 30 to 220) complex containing a single mutation of Nse4 and a 5'-FAM-labelled 37 bp dsDNA.

Fig. S9. A model for the Nse1-3-4 complex engaging with the Smc5/6 head regions in the nucleotide-free state.

(left) Models of Smc5 (pink N-lobe and magenta C-lobe domain) and Smc6 (white N-lobe and gray C-lobe) head domains (ATP-free state) generated by Phyre2 using the structure of condensin (PDB 6YVU) [9, 10]. Residues crosslinking Smc5 and Smc6 are shown as spheres in the circle, and all distances between these residues are shorter than 27 Å [7]. Residues in Smc5 and Smc6 that crosslink with the Nse1-3-4 complex are shown as yellow spheres. (right) Structure of the Nse1-3-4 complex in cylinder representation showing Nse1 (orange), Nse3 (green), and Nse4 (blue). Ser241 and Gln248 of Nse1 (yellow spheres) are positioned between the WHA and WHB of Nse1. The crosslinked residues between Smc5/6 and the Nse1-3-4 complex are connected by dashed lines [7]. Residues in human Nse1, Nse3, and Nse4 equivalent to those of *Xl*NSE proteins are marked inside the parenthesis.

Fig. S10. A model of the SMC5/6 complex bound to ATP and DNA.

(a) Structure-based sequence alignment of kleisin N-tails in cohesin, condensin, SMC5/6, and bacterial SMC complexes. The alignment is centered on the first helix (NH1) of the HTH motif

of kleisin. The conserved hydrophobic residues in the NH1 helix and the positively charged residues are highlighted in yellow and blue, respectively. The mutated residues of Nse4 in the EMSA analysis are indicated with red stars above residues.

(b-c) Structural representation of kleisin N-tails in two different DNA-bound cohesin structures. (b) *Hs*Rad21 (magenta); (c) *Sp*Rad21 (cyan). The residues equivalent to Arg52 and Arg38 of Nse4 are shown as spheres in *Hs*Rad21 (Lys25 and Arg11) and *Sp*Rad21 (Lys25 and Lys11). Arg33 and Arg35 of Nse4 and their equivalent residues in *Sp*Rad21 follow the opposite direction to DNA, and the equivalent residues are disordered in *Hs*Rad21. DNA and SMC are colored light brown and white, respectively.

Supplementary information related to Fig. S9

A model of the Smc5-Smc6 head regions bound with Nse1-3-4

Using the structures of the Nse1-3-4 complex and condensin (PDB 6YVU) [10], and the CL-MS data [7], we built a model for the Smc5/6 complex in the ATP-free state. In the CL-MS experiment, in which full-length human Smc5, Smc6 and the Nse1-3-4 complex were crosslinked in the absence of ATP and DNA (referred to as CL-MS$^{SMC-NSE}$), the majority of crosslinks occur at the interfaces between Smc5 and Smc6 arms. Thus, Smc5/6 may adopt a rod-like shape. We built the Smc5 and Smc6 heads using Phyre2 [9] based on the structure of condensin (PDB 6YVU). In the CL-MS$^{SMC-NSE}$ data, Lys245 and Tyr246 in *Xl*Smc6 crosslinked with Asn168 and Ser170 in *Xl*Smc5. We modelled the Smc5/6 heads so that residues could be located 24–27 Å apart (Fig. S9, left circle).

In the CL-MS$^{SMC-NSE}$ data, most of the crosslinks between SMC and Nse1-3 occur between the Smc6 N-lobe and the Nse1 C-terminus. Because Ser241 and Gln248 of *Xl*Nse1 that crosslinked with Smc6 are disordered in our structure, we predicted the position of the two residues from CL-MS^{NSE} data. We placed Ser241 and Gln248 of *Xl*Nse1 within 20 Å from the Cα atoms of their crosslinking residues (Arg28, Lys151, Arg156, Thr161, Lys212, and Gln248 for Ser241; Arg28, Lys151, Ser160, Thr161 for Gln248) as shown in the spheres in Figure S9. Next, we docked the Nse1-3-4 complex with the Smc5-Smc6 heads by locating the Nse1 C-terminus near the Smc6 N-lobe (Lys146, Lys150, Lys194), positioning Glu177 of Nse3 near Smc5 (Lys171), and Nse4 (Gln156, Ser160) near Smc6 (Lys146) (Fig. S9). All crosslinking

residues are within 30 Å.

In a model of the ATP-free SMC-NSE complex, the WHA and WHB of Nse1 are located close to the SMC head. The WHB of Nse3 is nearer the SMC head domain than WHA, hence the H1'' helix of Nse4M may be located in close proximity to the HTH motif, which binds to the neck of Smc6 (Fig. 7c). We modelled the N-terminal HTH motif (PDB 3W6J) [6] and the C-terminal WH domain (PDB 4I99) [11] of Nse4 using Phyre2, and placed them near the neck of Smc6 and the head of Smc5, respectively, by structurally aligning with Brn1 in the budding yeast condensin complex (PDB 6YVU). The HTH motif (residues 30 to 104) and Nse4M (residues 108 to 181) can be connected by a three residues linker, whereas the WH domain (residues 219 to 289) and Nse4M can be connected by a 37-residues linker in our model (Fig. 7c).

References

1. Zabrady, K., Adamus, M., Vondrova, L., Liao, C., Skoupilova, H., Novakova, M., et al., (2016). Chromatin association of the SMC5/6 complex is dependent on binding of its NSE3 subunit to DNA. *Nucleic Acids Res*., **44**, 1064–1079.

2. Vondrova, L., Kolesar P., Adamus, M., Nociar, M., Oliver, A.W., Palecek, J.J., (2020). A role of the Nse4 kleisin and Nse1/Nse3 KITE subunits in the ATPase cycle of SMC5/6. *Sci. Rep*., **10**, 9694.

3. Hudson, J.J.R., Bednarova, K., Kozakova, L., Liao, C., Guerineau, M., Colnaghi, R., et al., (2011). Interactions between the Nse3 and Nse4 components of the SMC5-6 complex identify evolutionarily conserved interactions between MAGE and EID families. *PLoS One*, **6**, e17270.

4. Serrano, D., Cordero, G., Kawamura, R., Sverzhinsky, A., Sarker, M., Roy, S., et al., (2020). The Smc5/6 Core Complex Is a Structure-Specific DNA Binding and Compacting Machine. *Mol. Cell*, **80**, 1025–1038.e5.

5. Guerineau, M., Kriz, Z., Kozakova, L., Bednarova, K., Janos, P., Palecek, J.J., (2012). Analysis of the Nse3/MAGE-binding domain of the Nse4/EID family proteins. *PLoS One*, **7**, e35813.

6. Kamada, K., Miyata, M., Hirano, T., (2013). Molecular basis of SMC ATPase activation: role of internal structural changes of the regulatory subcomplex ScpAB. *Structure*, **21**, 581–594.

7. Adamus, M., Lelkes, E., Potesil, D., Ganji, S.R., Kolesar, P., Zabrady, K., et al, (2020).

Molecular insights into the Architecture of the human SMC5/6 complex. *J. Mol. Biol*., **432**, 3820–3837.

8. Baker, N.A., Sept, D., Joseph, S., Holst, M. J., McCammon, J.A., (2001). Electrostatics of nanosystems: application to microtubules and the ribosome. *Proc. Natl. Acad. Sci. U.S.A*., **98**, 10037–10041.

9. Kelley, L.A., Mezulis, S., Yates, C.M., Wass, M.N., Sternberg, M.J., (2015). The Phyre2 web portal for protein modeling, prediction and analysis. *Nat. Protoc.*, **10**, 845–858.

10. Lee, B.G., Merkel, F., Allegretti, M., Hassler, M., Cawood, C., Lecomte, L., et al., (2020). Cryo-EM structures of holo condensin reveal a subunit flip-flop mechanism. *Nat. Struct. Mol. Biol.,* **27,** 743–751.

11. Bürmann, F., Shin, H.C., Basquin, J., Soh, Y.M., Giménez-Oya, V., Kim, Y.G., et al., (2013). An asymmetric SMC-kleisin bridge in prokaryotic condensin. *Nat. Struct. Mol. Biol.,* **20**, 371–379.

Supplementary Table

Table S1. Yeast strains used in this study

Name	Genotype
T275-2	*NSE4-13myc::HIS3*
T2186-7-1A	*nse4-H275E-13myc::HIS3*
T2187-45-1A	*nse4-R257E,H275E-13myc::HIS3*
T2191-27	*nse4-R251E,R256E,R257E,R258E,H275E,S276E-13myc::HIS3/+*
T2191-36	*nse4-K49E,R65E,R251E,R256E,R257E,R258E,H275E,S276E-13myc::HIS3/+*
X8563	*NSE4-13myc::HIS3/+*

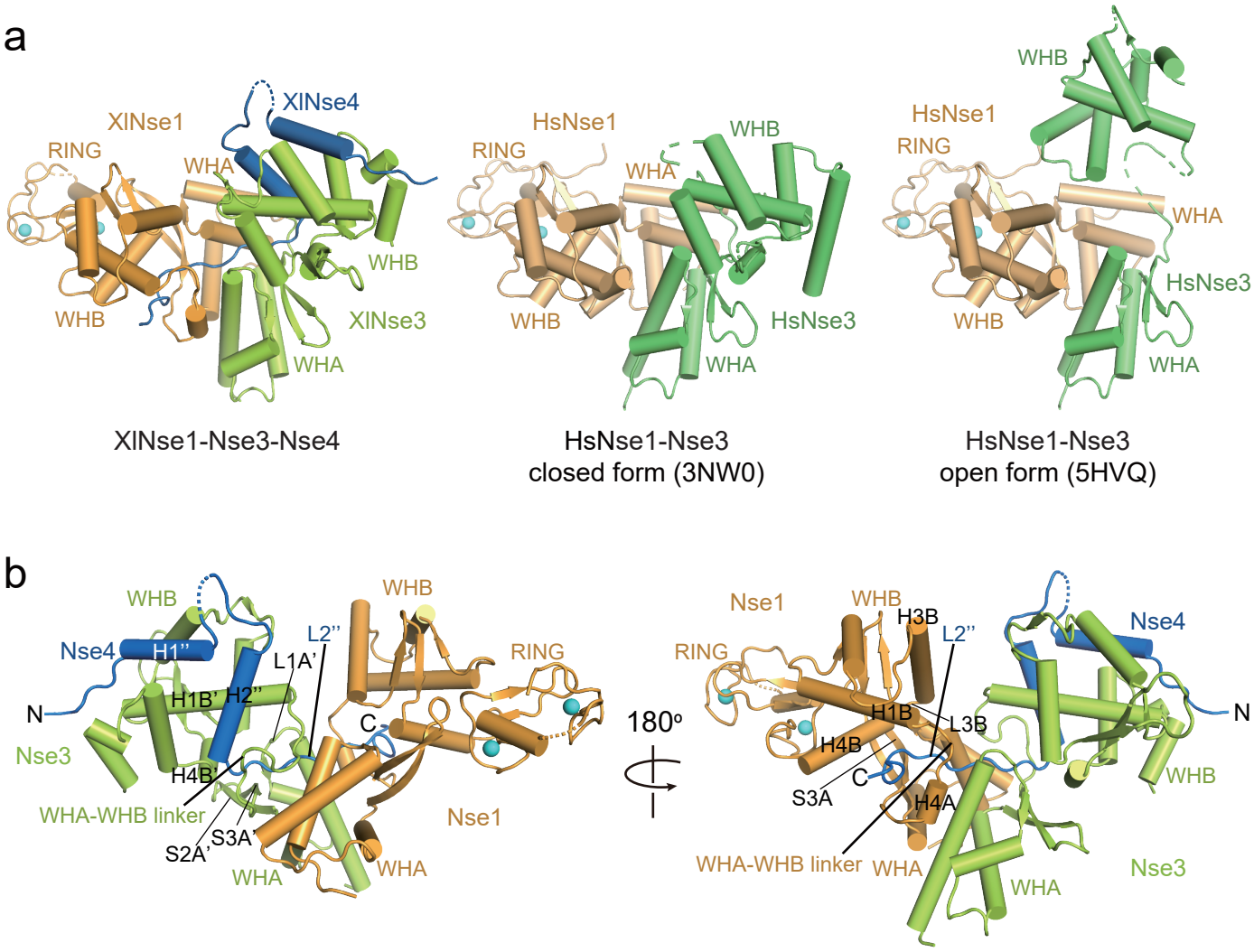
a
XlNse1
XlNse4
RING
WHA
WHB
WHB
XlNse3
WHA
XlNse1-Nse3-Nse4
HsNse1
WHB
RING
WHA
WHB
HsNse3
WHA
HsNse1-Nse3
closed form (3NW0)
WHB
HsNse1
RING
WHA
WHB
HsNse3
WHA
HsNse1-Nse3
open form (5HVQ)
b
WHB
WHB
Nse4
H1''
L2''
L1A'
RING
N
H1B'
H2''
C
Nse3
H4B'
WHA-WHB linker
S3A'
S2A'
Nse1
WHA
WHA
180°
Nse1
WHB
H3B
L2''
Nse4
RING
H1B
L3B
N
H4B
C
WHB
S3A
H4A
WHA-WHB linker
WHA
Nse3
WHA

Figure S1

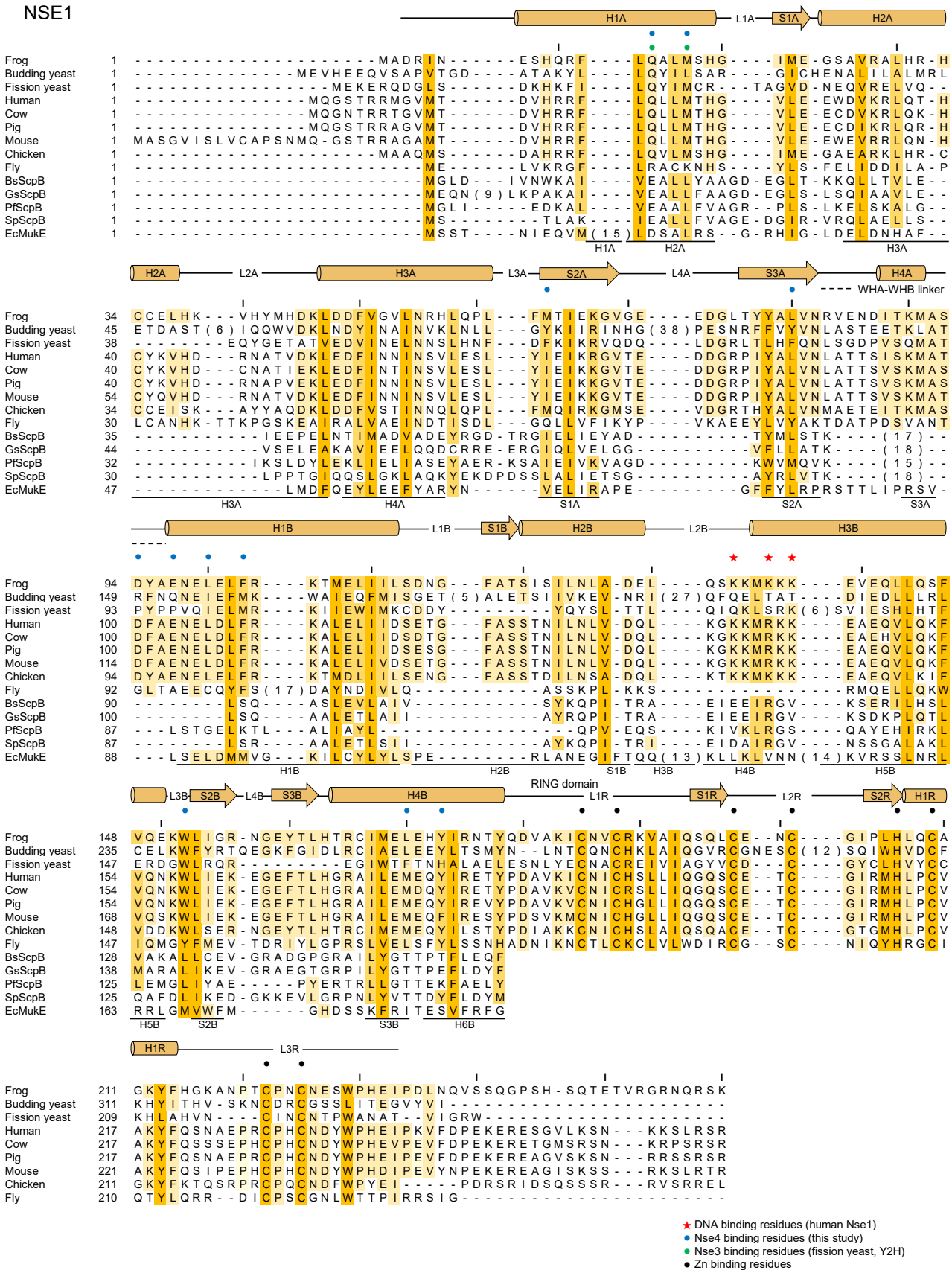
NSE1
H1A
L1A
S1A
H2A
Frog
Budding yeast
Fission yeast
Human
Cow
Pig
Mouse
Chicken
Fly
BsScpB
GsScpB
PfScpB
SpScpB
EcMukE
H2A
L2A
H3A
L3A
S2A
L4A
S3A
H4A
WHA-WHB linker
H1B
L1B
S1B
H2B
L2B
H3B
RING domain
L3B
S2B
L4B
S3B
H4B
L1R
S1R
L2R
S2R
H1R
L3R
H5B
H6B
DNA binding residues (human Nse1)
Nse4 binding residues (this study)
Nse3 binding residues (fission yeast, Y2H)
Zn binding residues

Figure S2

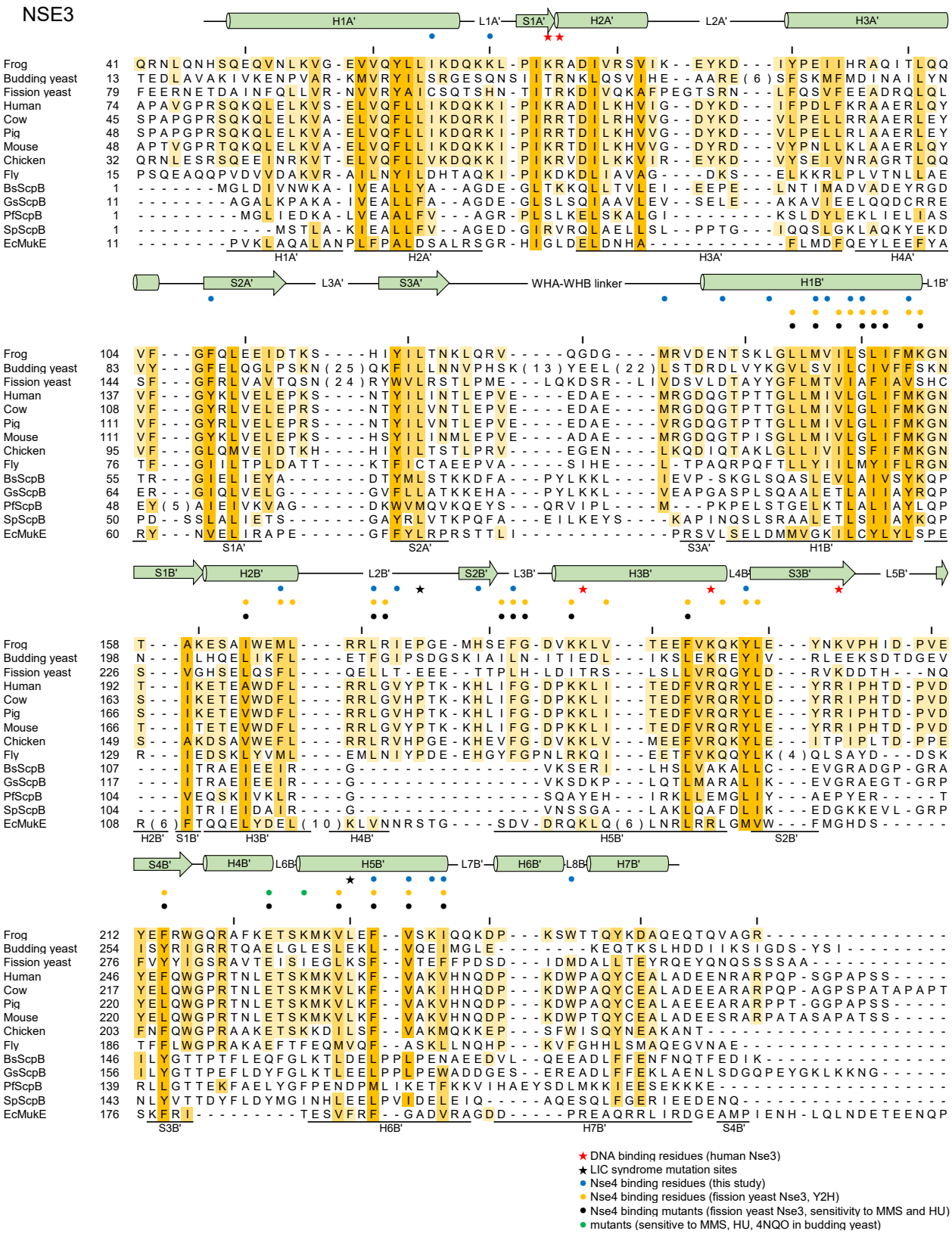
NSE3
H1A'
L1A'
S1A'
H2A'
L2A'
H3A'
Frog
Budding yeast
Fission yeast
Human
Cow
Pig
Mouse
Chicken
Fly
BsScpB
GsScpB
PfScpB
SpScpB
EcMukE
S2A'
L3A'
S3A'
WHA-WHB linker
H1B'
L1B'
S1B'
H2B'
L2B'
S2B'
L3B'
H3B'
L4B'
S3B'
L5B'
S4B'
H4B'
L6B'
H5B'
L7B'
H6B'
L8B'
H7B'
DNA binding residues (human Nse3)
LIC syndrome mutation sites
Nse4 binding residues (this study)
Nse4 binding residues (fission yeast Nse3, Y2H)
Nse4 binding mutants (fission yeast Nse3, sensitivity to MMS and HU)
mutants (sensitive to MMS, HU, 4NQO in budding yeast)

Figure S3

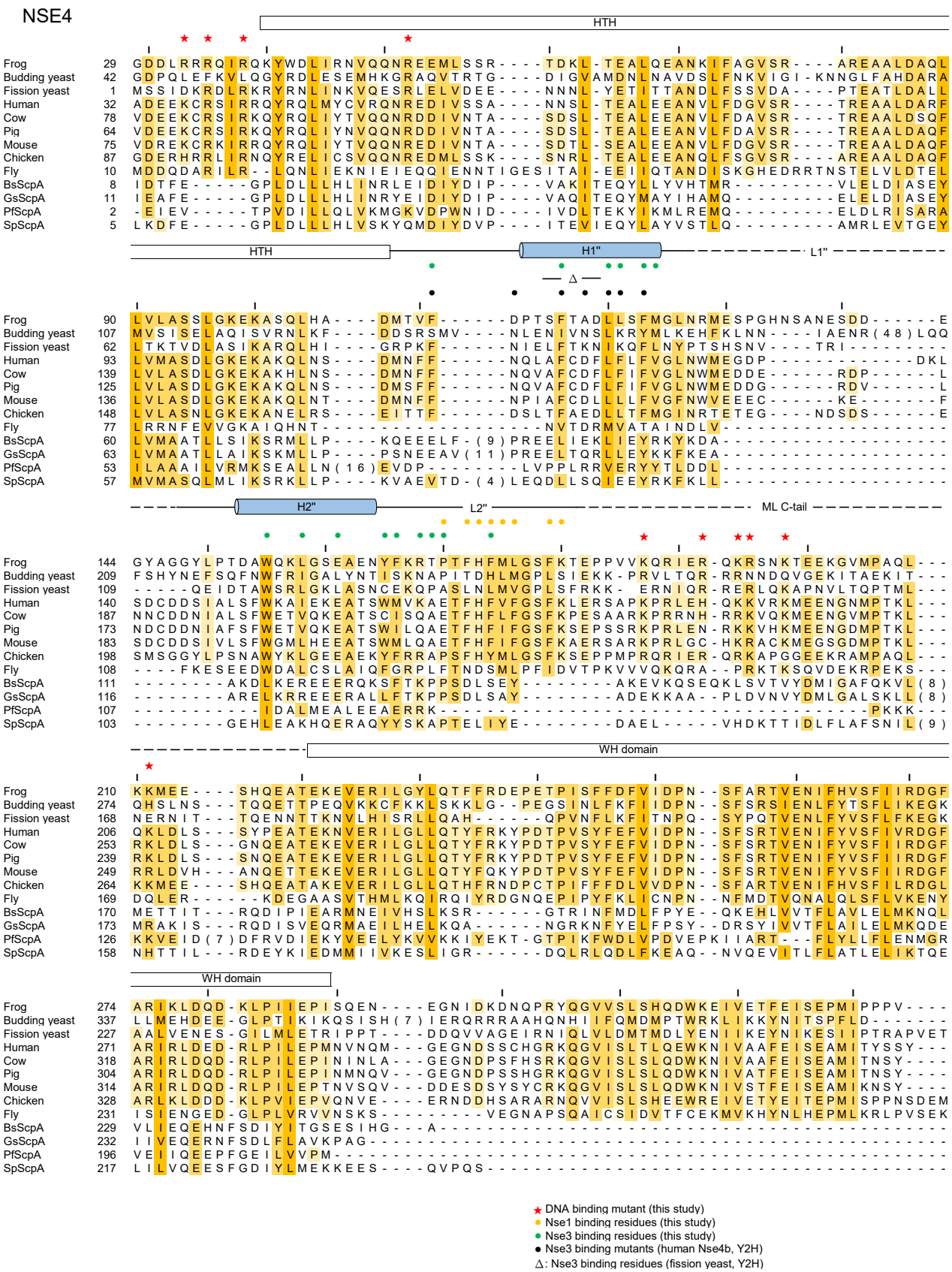
NSE4
HTH
HTH
H1"
L1"
H2"
L2"
ML C-tail
WH domain
WH domain
Frog
Budding yeast
Fission yeast
Human
Cow
Pig
Mouse
Chicken
Fly
BsScpA
GsScpA
PfScpA
SpScpA
★ DNA binding mutant (this study)
● Nse1 binding residues (this study)
● Nse3 binding residues (this study)
● Nse3 binding mutants (human Nse4b, Y2H)
△: Nse3 binding residues (fission yeast, Y2H)

Figure S4

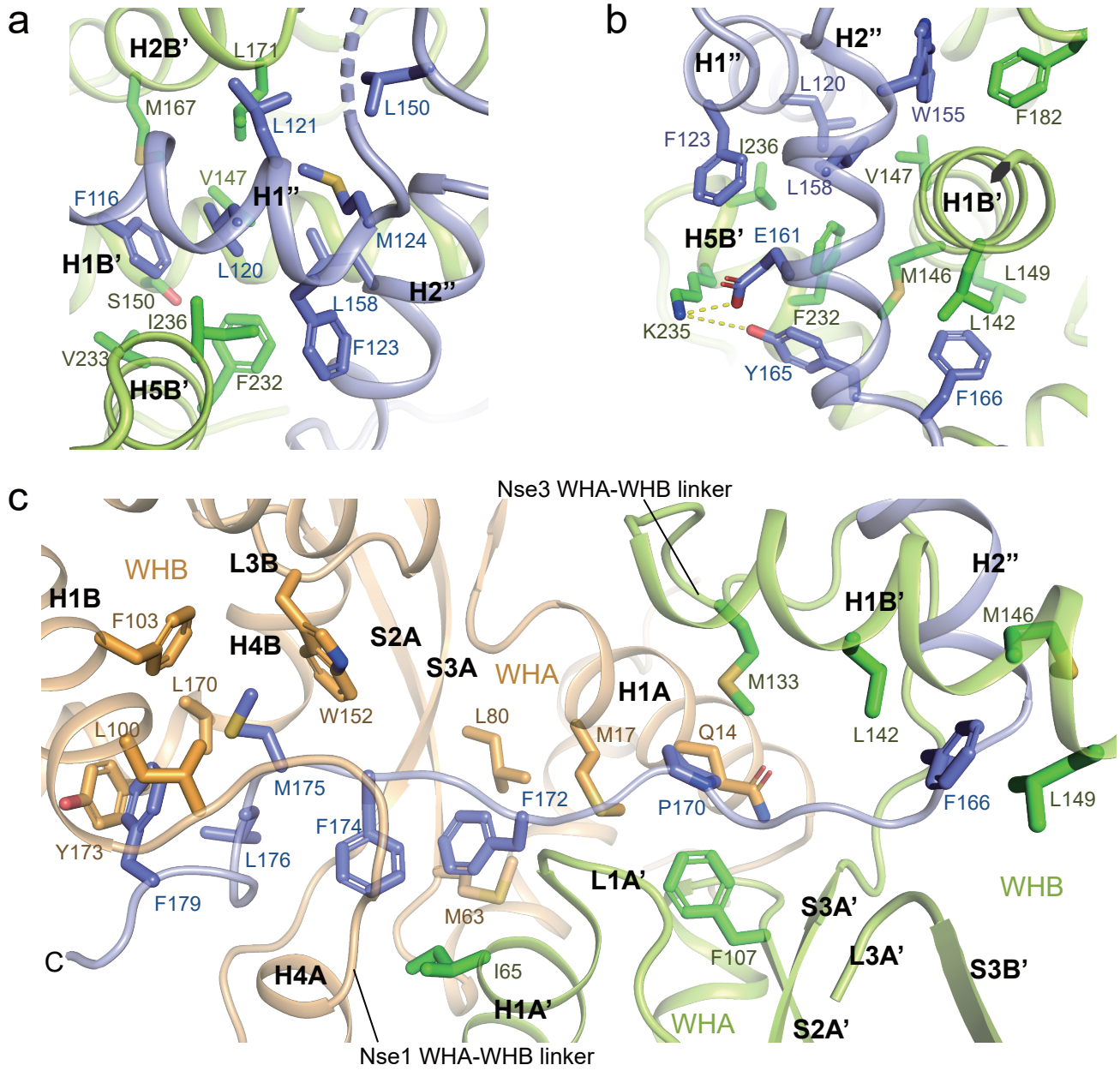
a
H2B'
L171
M167
L121
L150
V147
H1"
F116
M124
H1B'
L120
H2"
S150
L158
I236
F123
V233
H5B'
F232
b
H2"
H1"
L120
W155
F182
F123
I236
L158
V147
H1B'
H5B'
E161
M146
L149
K235
F232
L142
Y165
F166
c
Nse3 WHA-WHB linker
WHB
L3B
H1B
F103
H4B
S2A
S3A
WHA
H1A
H2"
H1B'
M146
M133
L170
W152
L80
M17
Q14
L142
L100
M175
F172
P170
F166
L149
F174
Y173
L176
L1A'
WHB
S3A'
F179
M63
F107
L3A'
S3B'
C
H4A
I65
H1A'
WHA
S2A'
Nse1 WHA-WHB linker

Figure S5

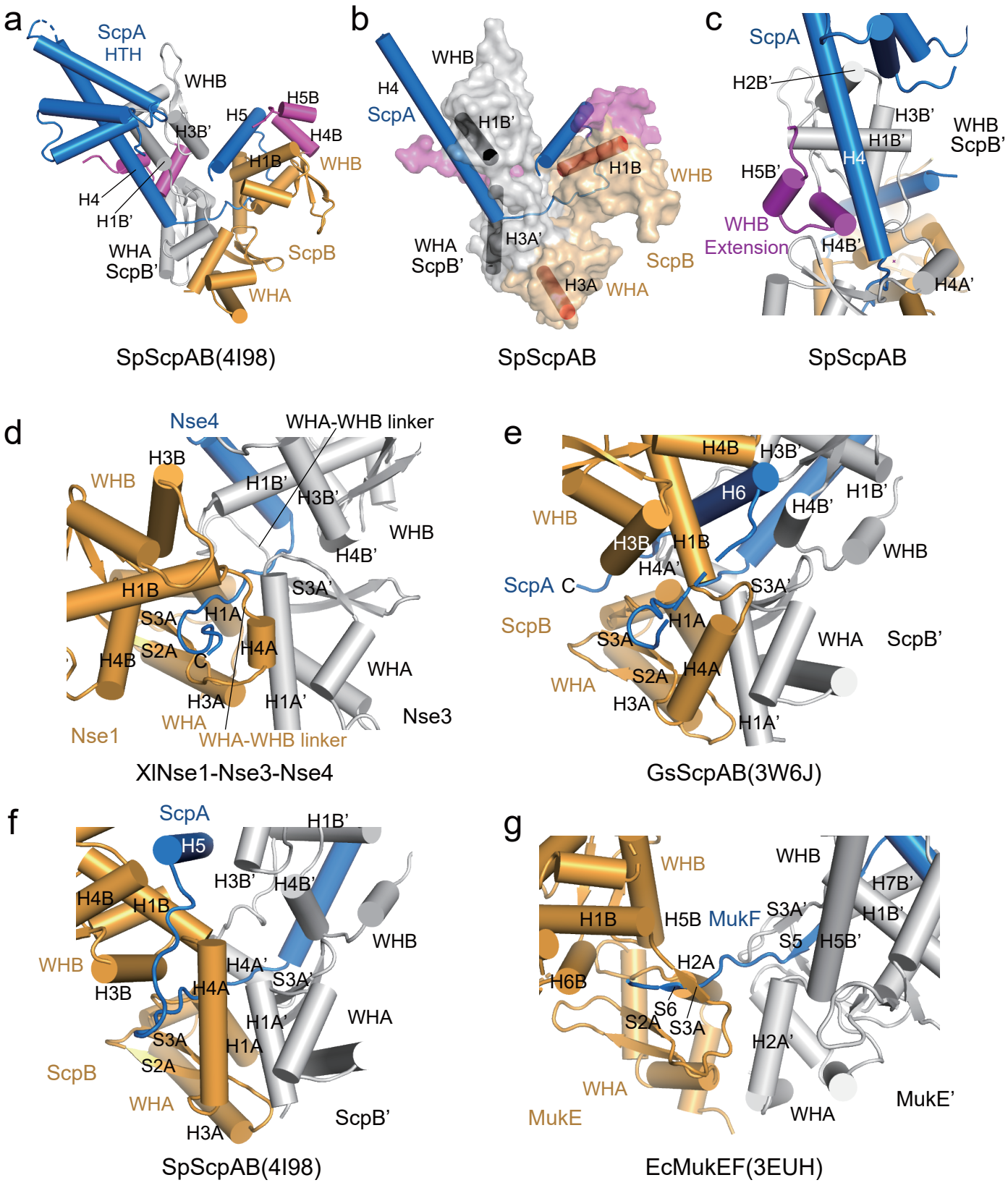
a
ScpA
HTH
WHB
H5B
H5
H3B'
H4B
H1B
WHB
H4
H1B'
WHA
ScpB'
ScpB
WHA
SpScpAB(4I98)
b
WHB
H4
ScpA
H1B'
H1B
WHB
WHA
ScpB'
H3A'
ScpB
H3A
WHA
SpScpAB
c
ScpA
H2B'
H3B'
WHB
ScpB'
H1B'
H4
H5B'
WHB
Extension
H4B'
H4A'
SpScpAB
d
Nse4
WHA-WHB linker
H3B
WHB
H1B'
H3B'
WHB
H4B'
H1B
S3A'
S3A
H1A
S2A
H4A
H4B
C
WHA
H3A
H1A'
WHA
Nse3
Nse1
WHA-WHB linker
XlNse1-Nse3-Nse4
e
H4B
H3B'
H6
H1B'
H4B'
WHB
H3B
H1B
WHB
H4A'
ScpA
C
S3A'
ScpB
H1A
S3A
WHA
ScpB'
WHA
S2A
H4A
H3A
H1A'
GsScpAB(3W6J)
f
ScpA
H1B'
H5
H3B'
H4B'
H4B
H1B
WHB
WHB
H4A'
S3A'
H3B
H4A
H1A'
WHA
S3A
H1A
S2A
ScpB
WHA
ScpB'
H3A
SpScpAB(4I98)
g
WHB
WHB
H7B'
H1B
H5B
MukF
S3A'
H1B'
S5
H5B'
H2A
H6B
S6
S2A
S3A
H2A'
WHA
MukE
WHA
MukE'
EcMukEF(3EUH)

Figure S6

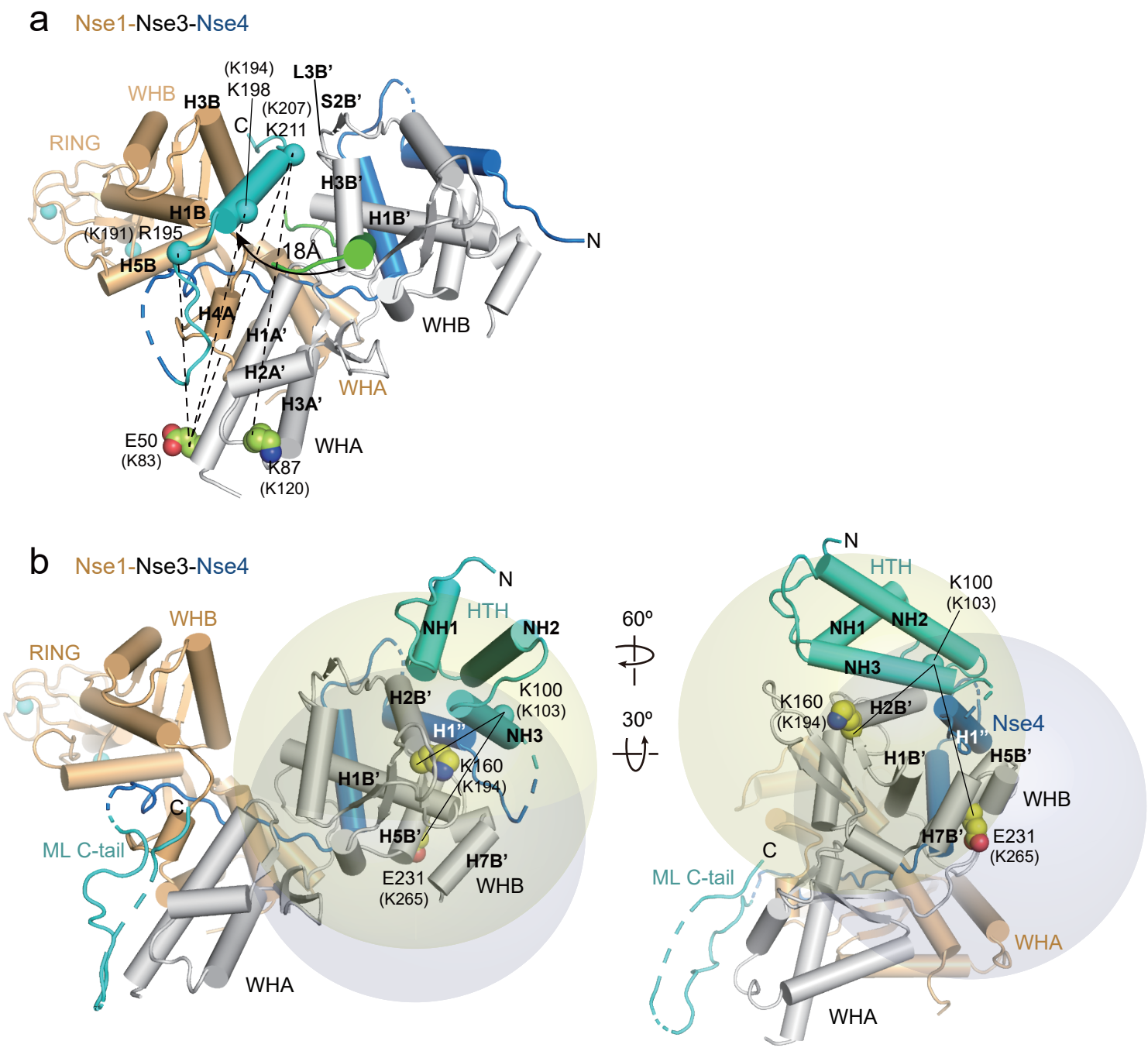
a
Nse1-Nse3-Nse4
(K194)
K198
L3B'
WHB
H3B
(K207)
S2B'
C
K211
RING
H3B'
H1B
H1B'
(K191) R195
N
18Å
H5B
H4A
WHB
H1A'
H2A'
WHA
H3A'
E50
(K83)
WHA
K87
(K120)
b
Nse1-Nse3-Nse4
N
HTH
WHB
RING
NH1
NH2
K100
(K103)
H2B'
H1"
NH3
K160
(K194)
H1B'
C
H5B'
ML C-tail
H7B'
E231
(K265)
WHB
WHA
60°
30°
N
HTH
K100
(K103)
NH1
NH2
NH3
K160
(K194)
H2B'
Nse4
H1"
H1B'
H5B'
WHB
H7B'
E231
(K265)
C
ML C-tail
WHA
WHA

Figure S7

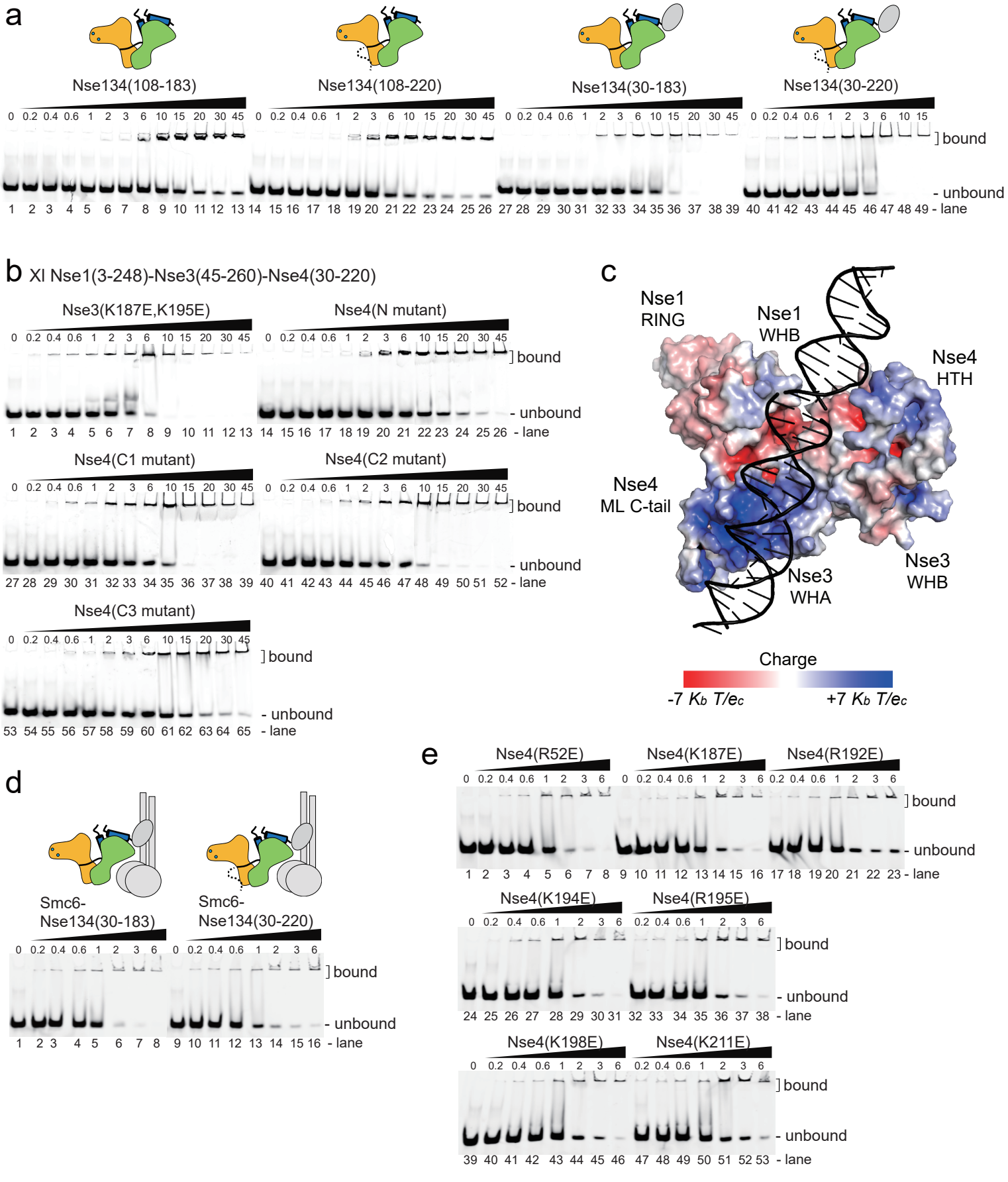
a
Nse134(108-183)
Nse134(108-220)
Nse134(30-183)
Nse134(30-220)
bound
unbound
lane
b XI Nse1(3-248)-Nse3(45-260)-Nse4(30-220)
Nse3(K187E,K195E)
Nse4(N mutant)
Nse4(C1 mutant)
Nse4(C2 mutant)
Nse4(C3 mutant)
c
Nse1 RING
Nse1 WHB
Nse4 HTH
Nse4 ML C-tail
Nse3 WHA
Nse3 WHB
Charge
-7 Kb T/ec
+7 Kb T/ec
d
Smc6-Nse134(30-183)
Smc6-Nse134(30-220)
e
Nse4(R52E)
Nse4(K187E)
Nse4(R192E)
Nse4(K194E)
Nse4(R195E)
Nse4(K198E)
Nse4(K211E)

Figure S8

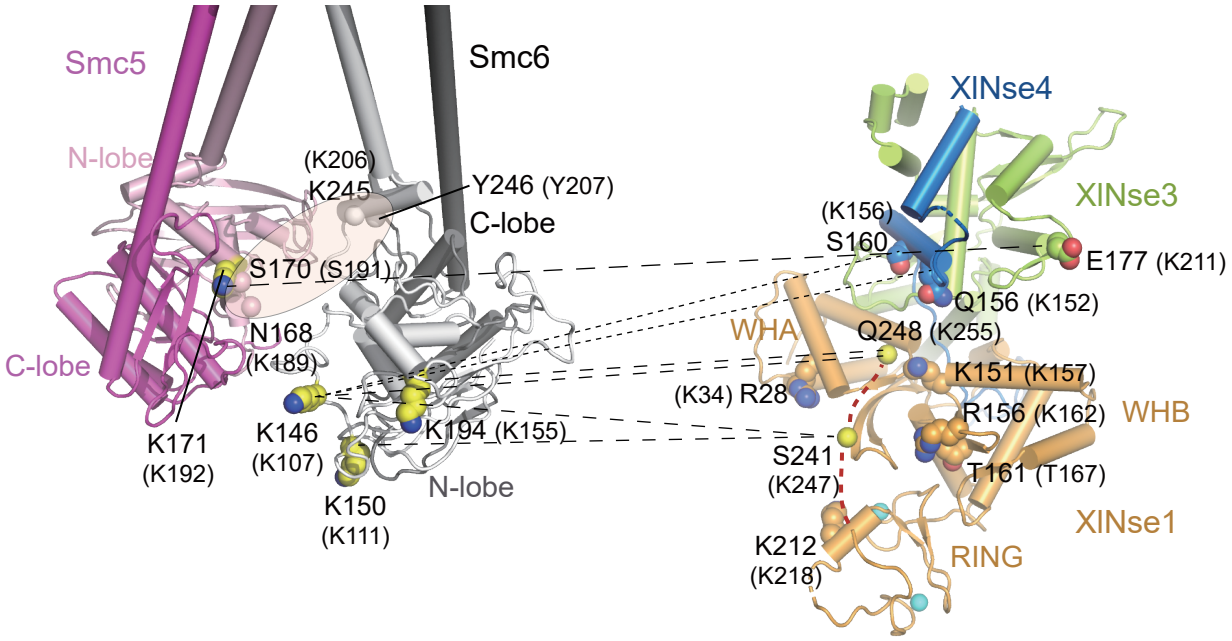
Smc5
Smc6
N-lobe
(K206)
K245
Y246 (Y207)
C-lobe
S170 (S191)
N168
(K189)
C-lobe
K171
(K192)
K146
(K107)
K194 (K155)
K150
(K111)
N-lobe
XlNse4
XlNse3
(K156)
S160
E177 (K211)
Q156 (K152)
WHA
Q248 (K255)
K151 (K157)
(K34) R28
R156 (K162)
WHB
S241
(K247)
T161 (T167)
XlNse1
K212
(K218)
RING

Figure S9

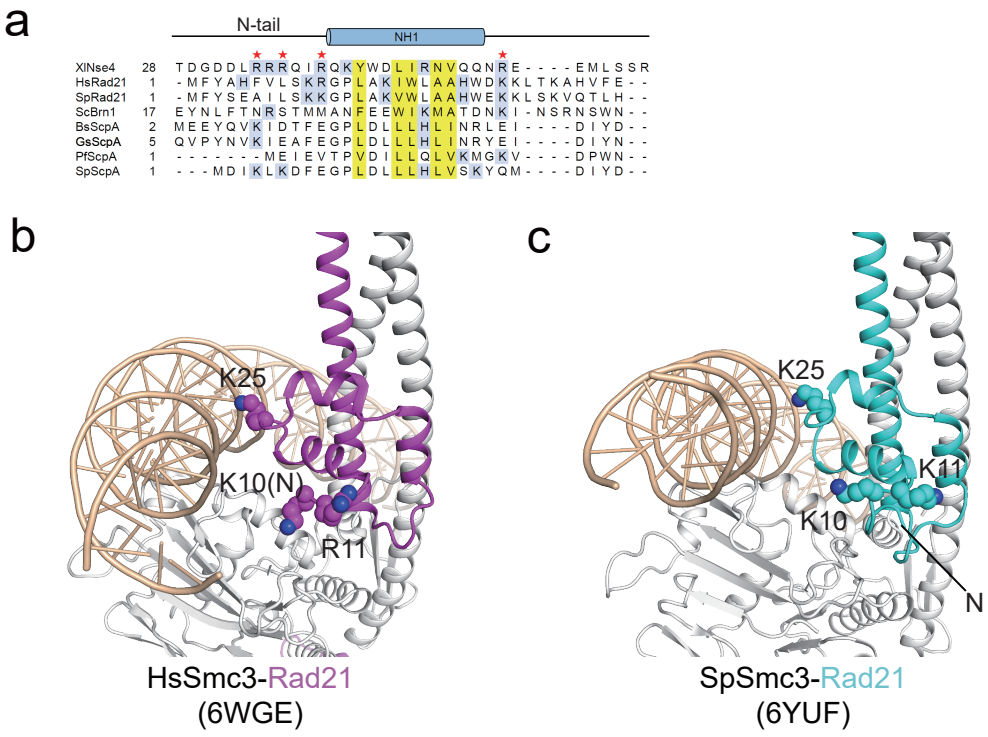
a
N-tail
NH1
XlNse4 28 TDGDDLRRRQIRQKYWDLIRNVQQNRE----EMLSSR
HsRad21 1 -MFYAHFVLSKRGPLAKIWLAAHWDKKLTKAHVFE--
SpRad21 1 -MFYSEAILSKKGPLAKVWLAAHWEKKLSKVQTLH--
ScBrn1 17 EYNLFTNRSTMMANFEEWIKMATDNKI-NSRNSWN--
BsScpA 2 MEEYQVKIDTFEGPLDLLLHLINRLEI----DIYD--
GsScpA 5 QVPYNVKIEAFEGPLDLLLHLINRYEI----DIYN--
PfScpA 1 -------MEIEVTPVDILLQLVKMGKV----DPWN--
SpScpA 1 ---MDIKLKDFEGPLDLLLHLVSKYQM----DIYD--
b
K25
K10(N)
R11
HsSmc3-Rad21
(6WGE)
c
K25
K11
K10
N
SpSmc3-Rad21
(6YUF)

Figure S10